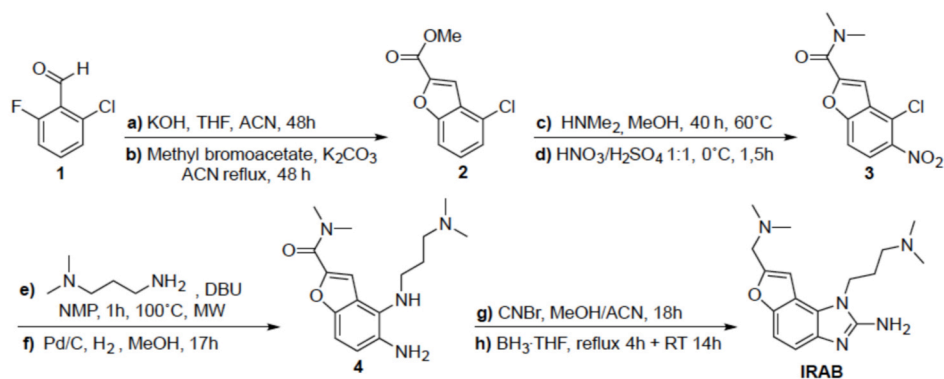


SUPPLEMENTARY FIGURES

Figure S1. Synthetic scheme for the preparation and characterization of IRAB.



Reaction yields: a) 45%; b) 58%; c) 91%; d) 31%; e) 83%; f and g) 77%; h) 34%

Characterization of IRAB

mp : 150-152°C

¹H-RMN (D₂O, 400 MHz) δ (ppm): 7.63 (d, ³J=8.8 Hz, 1H, H₈), 7.51 (d, ³J=8.8 Hz, 1H, H₇), 7.50 (s, 1H, H₁₁), 4.66 (s, 2H, H₁₃), 4.48 (t, ³J=8.8 Hz, 2H, H₄), 3.32 (m, 2H, H₂), 3.00 (s, 6H, H₁), 2.88 (s, 6H, H₁₄), 2.38 (m, 2H, H₃).

¹³C-RMN (D₂O, 100 MHz) δ (ppm): 153.40 (C₅), 149.46 (C₁₂), 147.54 (C₉), 124.05 (C₇), 122.17 (C₆), 111.81 (C₁₅), 109.60 (C₁₀), 107.94 (C₈), 106.50 (C₁₁), 54.12 (C₁₃), 53.07 (C₂), 42.66 (C₁), 42.24 (C₁₄), 40.70 (C₄), 23.32 (C₃).

HRMS (ESI, positive mode) *m/z*: 316.2134 [M+H]⁺, calculated mass for C₁₇H₂₅N₅O: 315,2059 [M]

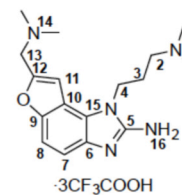


Figure S2. Lack of inhibitory effect of peptoids (A) and PNAs (B) on the *in vitro* translation efficiency driven by the FMDV IRES. The chemical structure of peptoids A9, A10, and PNAs E24 and E27 is shown on top of the autoradiography of translation products (luc and CAT) synthesized in reticulocyte lysates using the FMDV bicistronic RNA incubated with the indicated amounts of these compounds.

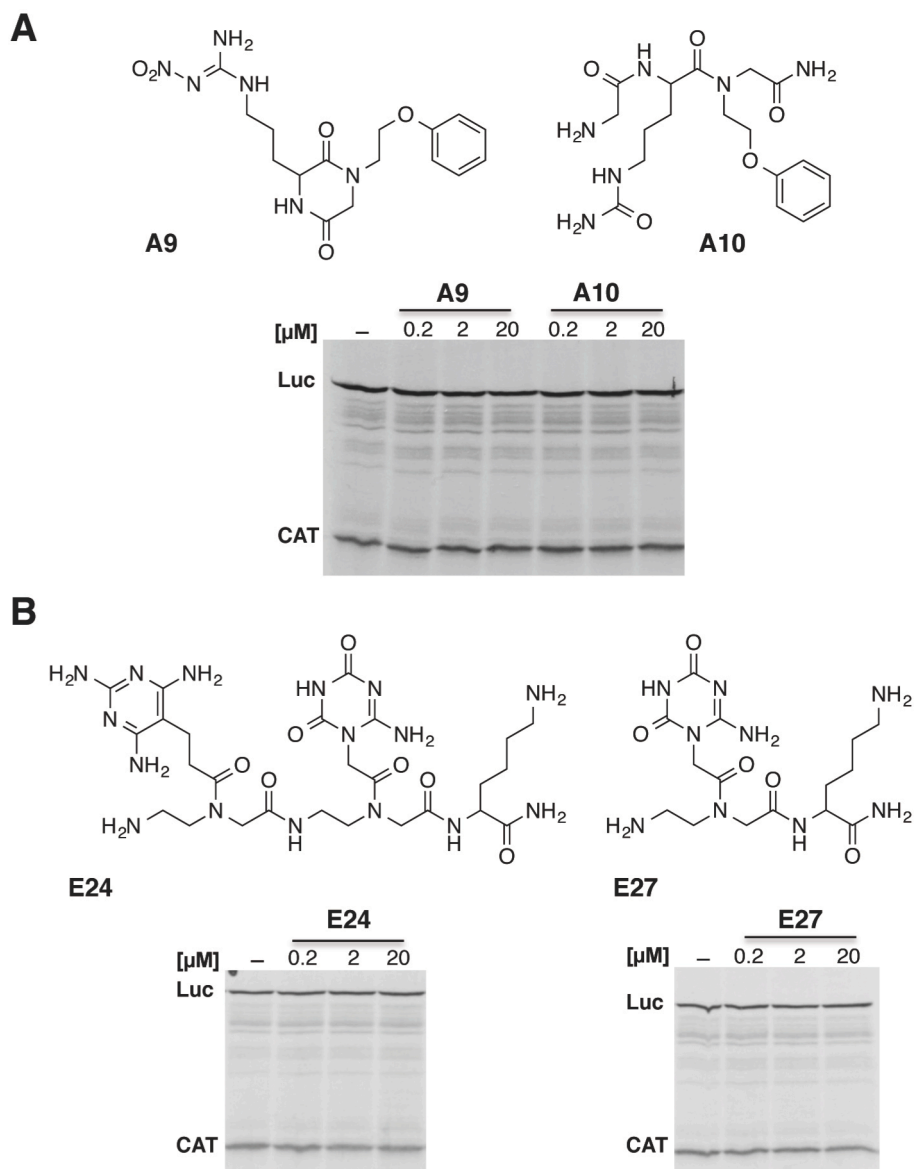


Figure S3. Inhibitory effect of IRAB on the *in vitro* translation efficiency driven by the HCV IRES. (A) Autoradiography of translation products synthesized in reticulocyte lysates using the HCV bicistronic RNA incubated with the indicated amounts of IRAB. The intensity of Luc and CAT polypeptides in each lane were determined by densitometry and made relative to the total intensity of the lane with DMSO alone, which was set at 100%. Data corresponds to the mean (\pm SD) of three independent assays. (B) **Inhibitory effect of Isis-11 on the *in vitro* translation efficiency. Autoradiography of translation products obtained from *in vitro* synthesized HCV RNA in the presence of the indicated amounts of Isis-11. The intensity of the lanes were determined by densitometry and made relative to the total intensity of the lane with DMSO alone, which was set at 100%. Data corresponds to the mean (\pm SD) of three independent assays.**

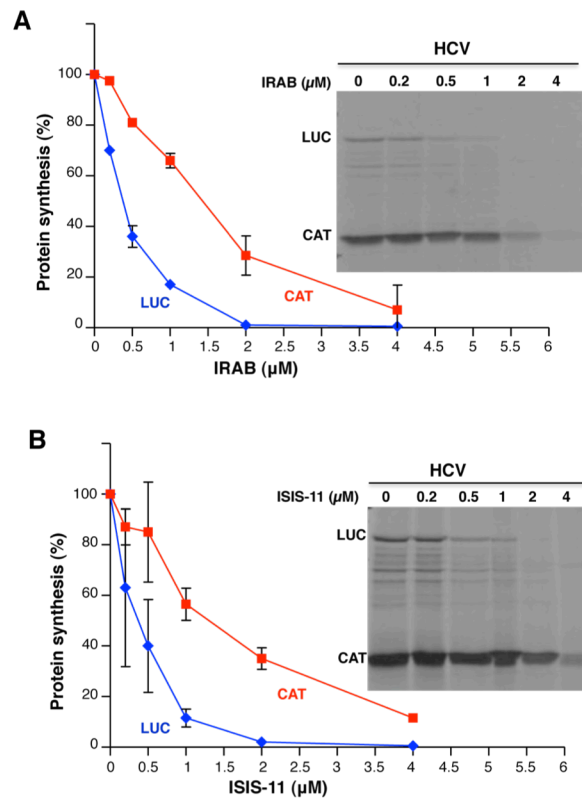


Figure S4. Inhibitory effect of IRAB on the *in vitro* translation efficiency driven by the HCV IRES. (A) Autoradiography of translation products synthesized in reticulocyte lysates using a monocistronic RNA incubated with the indicated amounts of IRAB or Isis-11. (B) The intensity of Luc polypeptide in each lane was determined by densitometry and made relative to the total intensity of the lane with DMSO alone, which was set at 100%. Data corresponds to the mean (\pm SD) of three independent assays.

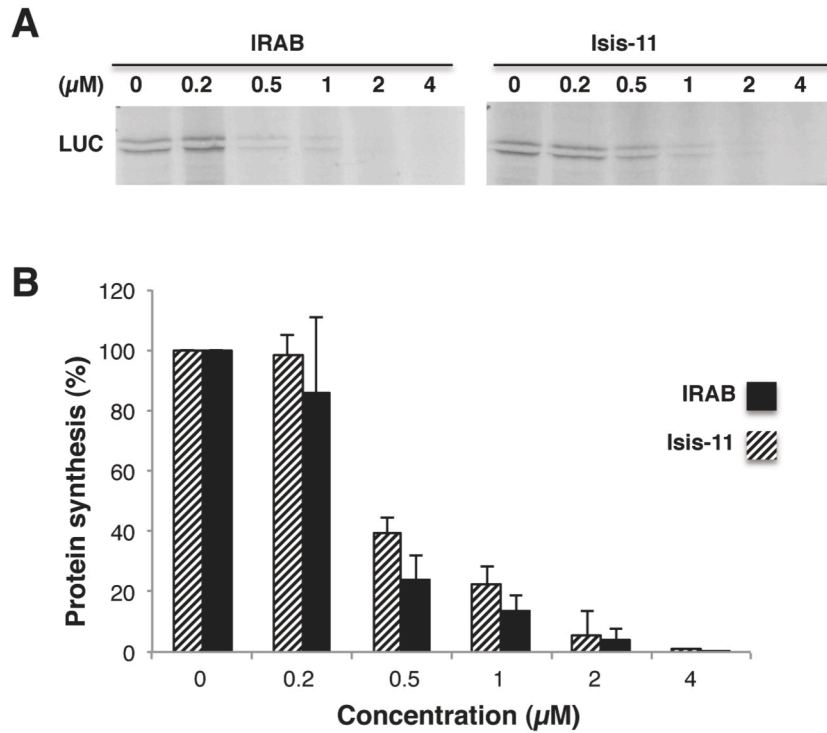


Figure S5. Effect of IRAB and Isis-11 on cell growth. **A.** Cell viability upon Isis-11 or IRAB treatment relative to untreated cells. Cells were seeded in DMEM supplemented with FCS in the absence or presence of IRAB and Isis-11 (1 or 2 μM). At the indicated times, the number of cells/ml (mean \pm SD) was determined using a Neubauer chamber. **B.** Cells treated with the indicated concentrations of IRAB or Isis-11 were used to determine detachment of the monolayer by crystal violet staining 48 hrs after.

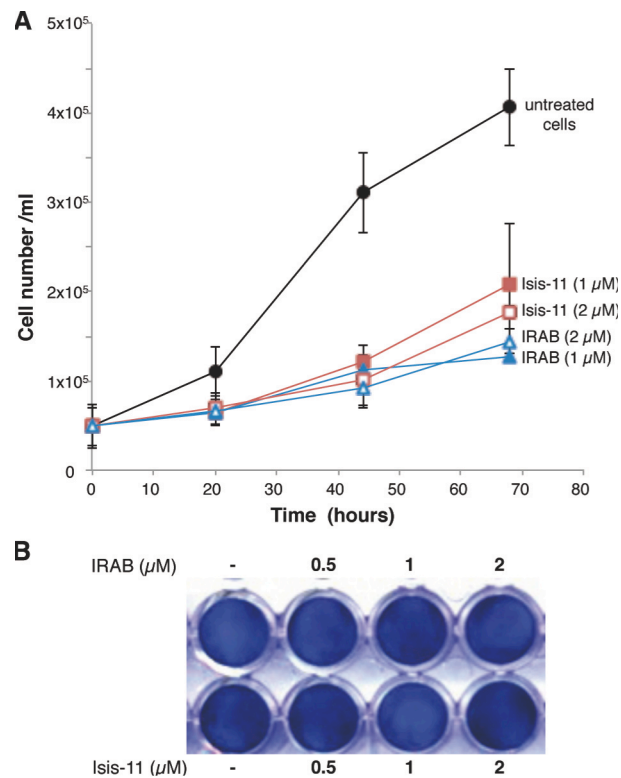


Figure S6. Modification of SHAPE reactivity profile upon incubation of the IRES RNA with increasing amounts of IRAB. SHAPE reactivity profiles of the IRES folded at 0.5 mM Mg²⁺ (free RNA) or in the presence of IRAB (2, 10, 20 μM). SHAPE reactivity is represented in a colored scale in which 0 indicates unreactive nucleotides and the average intensity at highly reactive nucleotides is set to 1.0. Nucleotide positions are indicated on the x-axis. Domains 1, 2, 3, 4 and 5 of the IRES are indicated below the corresponding nt position. A broken rectangle depicts the region harboring main reactivity changes.

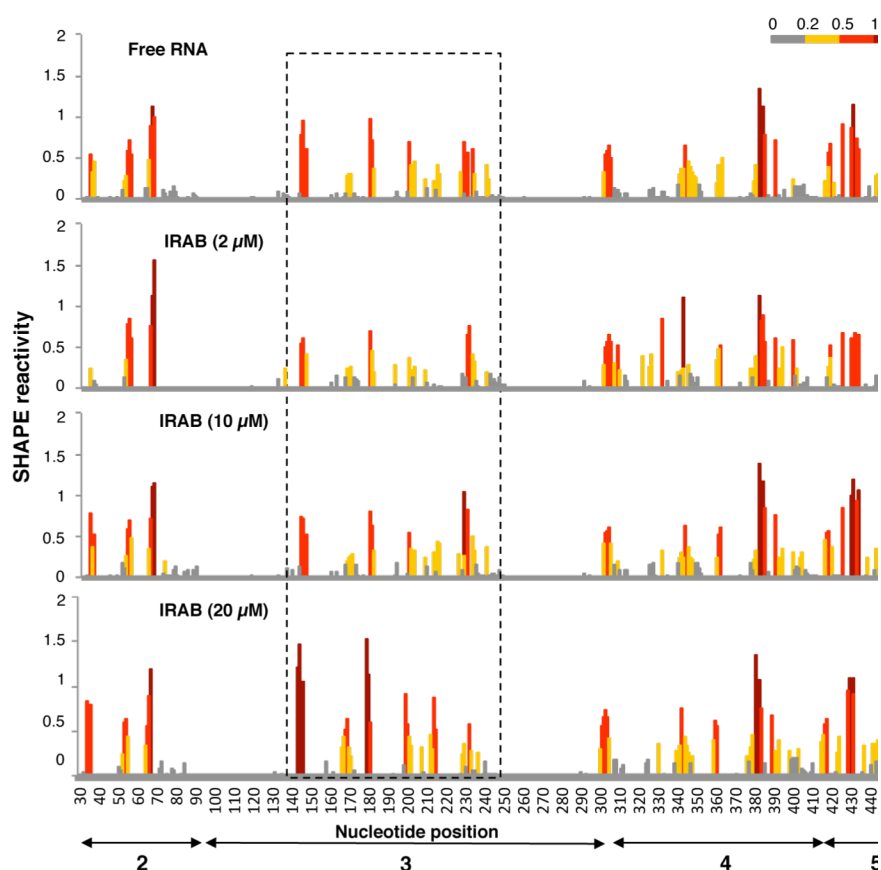


Figure S7. Dose-response curves corresponding to the titration of 0.5 mM AP54 with IRAB (top) and Isis-11 (bottom). Excitation wavelength 310 nm.

